ChemComm

COMMUNICATION

View Article Online
View Journal | View Issue

Cite this: *Chem. Commun.*, 2018, **54**, 6947

Received 29th May 2018,
Accepted 31st May 2018

DOI: 10.1039/c8cc04292f

rsc.li/chemcomm

Framework *vs.* side-chain amphidynamic behaviour in oligo-(ethylene oxide) functionalised covalent-organic frameworks†

Demetrius A. Vazquez-Molina,[a] Giovanna M. Pope,[a] Andrew A. Ezazi,[a] Jose L. Mendoza-Cortes,*[bcd] James K. Harper*[a] and Fernando J. Uribe-Romo*[a]

We present a family of covalent organic frameworks that have been functionalized with oligo-(ethylene oxide) chains of varying lengths. Because of the open structure of the COFs, the side chains do not interfere with their crystallization obtaining materials with predictable crystal structure. The difference in length of the side-chains allowed for the determination of amphidynamic behaviour with the use of ^{13}C solid-state NMR relaxation methods. Computational calculations further contribute to understanding the atomistic dynamic behaviour of the different atoms. This study demonstrates the ability to design complex behaviour in organic crystals.

One of the most outstanding challenges in the field of organic crystalline materials is the ability to systematically control molecular dynamic behaviour in the solid state.[1] This challenge arises from the inability to control the crystalline packing of amphidynamic molecules. These molecules exhibit contrasting fast and slow molecular movement within the same molecule, and are the base for the development of molecular machines that operate in the solid state.[2] Garcia-Garibay[3] has elegantly shown that amphidynamic molecules can be designed by synthetically creating a pocket of free volume within a molecule, so that free rotation in a rigid lattice can occur. As the crystalline packing of molecules cannot be accurately controlled,[4] the presence of this free volume cannot be easily accessed without lengthy synthetic routes. This inhibits the rapid preparation of amphidynamic materials in a modular way.

Covalent-organic frameworks (COFs) are crystalline organic materials formed by building blocks that assemble into predictable topologies creating large amounts of free volume (or pores).[5] The presence of large pores alleviates steric constraints, allowing for the organization of the building blocks into crystalline packings that retain the same arrangements as the unfunctionalised COFs, including space groups, which has been proven true in most cases.‡[6] This means that COFs should diffract with the same X-ray powder pattern regardless of the type of functionalization, making characterization of new materials straightforward. These features inspired us to systematically study the amphidynamic behaviour of COFs that have been functionalized with flexible oligo-(ethylene oxide) (OEO) side-chains of varying lengths.

An unfunctionalised 2-dimensional COF is typically composed by rigid 2-connected molecular struts that are linked to divergent nodes through covalent bonds, forming infinite layers that stack like graphite.[7] This packing creates 1-dimensional channels that can host highly dynamic processes. In a previous report,[8] we demonstrated that ions such as Li^+ can be incorporated as guests in unfunctionalised COFs, exhibiting high ionic conductivity under electrochemical potentials. This inspired us to further study enhancing the dynamics of the pore through chemical ways. Here, we functionalized the pores of COF with groups that can enable lithium mobility. These groups are OEO chains that render the pore with a similar environment as poly-(ethylene oxide) electrolyte gels, where the oxygen atom in the ether can enhance the movement of lithium.[9] We hypothesized that COFs functionalized with highly mobile OEO chains can produce tuneable amphidynamic behaviour. This strategy will enhance guest transport within the pore and allow us to study the structure–property relationships of amphidynamic COFs.

We prepared a family of β-keto-enamine COFs based on the condensation of 4,4″-diamino-*p*-terphenyl, **TP-R** organic strut with 1,3,5-triformyl-phloro-glucinol, **Tfp** (Fig. 1A),[10] where the central ring in **TP** was decorated with oligo-(ethylene oxide) groups that include ethoxy (R = **OEt**), ethylene glycol monomethyl ether (**OMEG**), diethylene glycol monomethyl ether (**ODEG**), and triethylene glycol monomethyl ether (**OTEG**). This type of functionalization is readily

[a] *Department of Chemistry, University of Central Florida, 4111 Libra Dr Orlando, FL 32816, USA. E-mail: james.harper@ucf.edu, fernando@ucf.edu*
[b] *Department of Chemical & Biomedical Engineering, Florida A&M – Florida State University, Joint College of Engineering, 2525 Pottsdamer Street, Tallahassee, Florida, 32310, USA. E-mail: mendoza@magnet.fsu.edu*
[c] *Department of Physics, Scientific Computing, Materials Science and Engineering, High Performance Materials Institute, Florida State University, Tallahassee, Florida, 32310, USA*
[d] *Condensed Matter Theory, National High Magnetic Field Laboratory (NHMFL), Florida State University, 1800 E. Paul Dirac Drive, Tallahassee, Florida, 32310, USA*

† Electronic supplementary information (ESI) available: Includes detailed synthetic procedures, crystal models, NMR data and MD simulations. See DOI: 10.1039/c8cc04292f

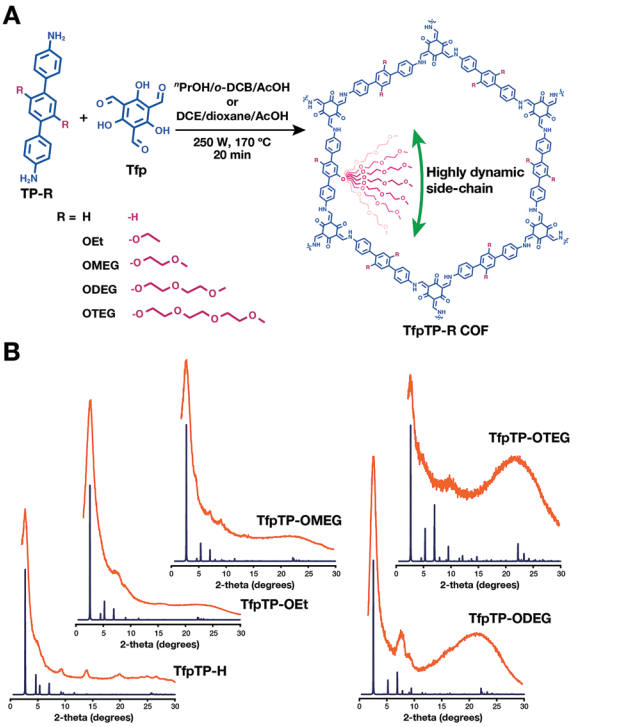

Fig. 1 (A) Reaction scheme for the synthesis of amphidynamic β-ketoenamine COFs. Static framework is highlighted in blue and mobile side-chains in red. (B) Powder X-ray diffraction patterns of the prepared amphidynamic COFs. Orange trace is experimental pattern; blue trace is the simulated powder pattern from the respective crystal model (ESI†).

accessible because of the facile synthesis of the building blocks. Moreover, the uniform type of signals to be observed using solid-state NMR relaxation techniques allowed us to easily measure and understand the differences in amphidynamic behaviour between the framework and the side-chain. We prepared building blocks **TP-R** (Fig. 1A) *via* S_N2 reaction between 1,4-dibromohydroquinone and the respective OEO monomethyl ether tosylate (or iodoethane for **TP-OEt**), followed by Suzuki coupling with 4-amino-phenyl-boronic pinacol ester (ESI†). Reaction of the respective monomers with **Tfp** under solvothermal conditions using a microwave reactor (250 W) in a solvent mixture of either 17 : 17 : 1 (v/v/v) 1,2-dichloroethane/dioxane/acetic acid 8 M (aq) for **TfpTP-H** and **TfpTP-OEt**, or 17 : 17 : 1 (v/v/v) *n*-propanol/1,2-dichlorobenzene/acetic acid 8 M (aq) for **TfpTP-OMEG**/**TfpTP-ODEG**/**TfpTP-OTEG**, at 170 °C for 20 min produced the crystalline COFs in high yields (Fig. 1). The unfunctionalised COF with R = H (**TfpTP-H**) was also prepared as a reference to quantify the dynamics of the framework itself.[11]

Powder X-ray Diffraction (PXRD, Cu Kα radiation) of the prepared COFs displayed the expected (100) peak at 2.6 degrees (2θ), with high intensity followed by the low-intensity (110), (200), (210), and the broad (001) peak at 23.1 degrees evidencing successful crystallization of the COFs. The fact that all the prepared materials exhibit the same diffraction peaks demonstrates their isoreticular nature. Crystal modelling of the respective COFs using Materials Studio Modelling Suite[12] allowed for the prediction of their crystal packing in the hexagonal *P6*/*m* space group. In those models, the functional groups are inside of the pore and will not affect the packing of the crystal, so the crystallographic cell parameters remain almost invariant among the models (Table S1, ESI†). Therefore, all COFs are expected to exhibit diffraction patterns with peaks at the same diffraction angles. The only variation observed was a subtle difference in the intensity of the simulated peaks, as it can be appreciated in Fig. 1B (blue traces). In these models, the side-chains are locked in defined crystallographic positions influencing the distribution of electron density in the crystal (and thus the intensity of the peaks). We observed that the experimental patterns do not follow the predicted changes in intensity. This is possible because the side-chains in the prepared COFs are not located in well-defined positions, *i.e.*, are disordered. Crystallography theory states that disordered atoms in a unit cell can be the result of positional disorder, dynamic disorder, or a combination of both.[13] Thus, time-averaged crystallography cannot differentiate between the dynamic and static mechanism for atomic disorder.

Solid-state NMR on the other hand, is a time-resolved technique that provides dynamic information for nuclei of interest. This information is contained in the spin–lattice relaxation constant (T_1) that reflects the loss of nuclear magnetization caused by the dynamic behaviour of the nuclei. Therefore, this T_1 spin–lattice relaxation is related to molecular mobility.[14] While ^{1}H T_1 is usually the same for all sites in a unit cell, measurements of ^{13}C T_1 provides site resolved information. Thus, measurement of T_1 constants, provide insight into the amphidynamic behaviour between carbon nuclei in the framework and ^{13}C sites in the side-chains. The cross polarization with magic angle spinning (CP-MAS) NMR spectra of the COF series display signals that correspond to aromatic, carbonyl, and imine framework carbon atoms between 100 and 160 ppm for all COFs, including **TfpTP-H** (Fig. 2A). Addition of oligo-(ethylene oxide) chains results in an appearance of two signals between 0 and 80 ppm. The signal at around 75 ppm corresponds to –CH_2– methylene carbons and the lower frequencies signals correspond to the –CH_3 methyl carbon. Determination of the T_1 constants was performed using the saturation-recovery pulse sequence which relates the intensity I of a peak at an arbitrary recovery time t with the following equation:

$$I = I_o\,(1 - e^{-t/T_1}) \qquad (1)$$

where I_o is the intensity of the peak at infinite recovery times. The saturation recovery experiment for aromatic and side-chain carbons of **TfpTP-OTEG** is shown in Fig. 2B, displaying the very different shapes caused by notably different spin–lattice relaxation times. Framework carbons exhibited large values, whereas side-chain carbons displayed low values. Plotting the T_1 relaxation times for all the carbons in the prepared COFs (Fig. 3) clearly illustrates that side chain carbons experience significantly more motion than framework positions. Length of side chain is also important, with **TfpTP-OEt** COF showing a relatively slow relaxation of the CH_2 carbon (7.7 s). By simply extending the chain length by a OCH_3 group (*i.e.*, **TfpTP-OMEG**), the CH_2 relaxation decreases almost by six-fold, implying that the length of the chain plays a significant role in its dynamics. Moreover, extending chain length further to **ODEG** and **OTEG** increases the region experiencing amphidynamic properties, but the side chain T_1-data suggests that the mobility of **OMEG**, **ODEG** and

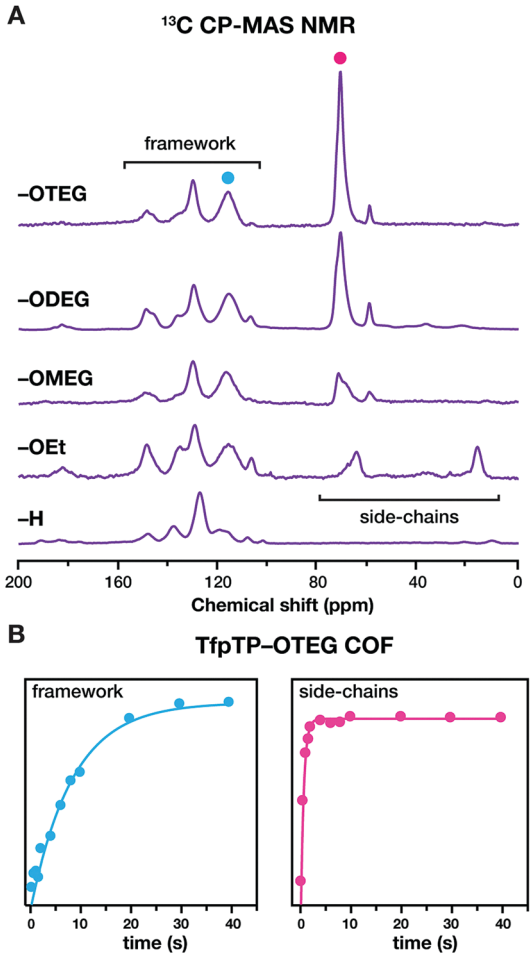

Fig. 2 (A) ^{13}C CP-MAS spectra of the prepared COFs (spinning rate 12 kHz). (B) Time evolution saturation-recovery plots for **TfpTP-OTEG** including fitted function from eqn (1). The colour of the data points indicates their signal in the 1D spectrum.

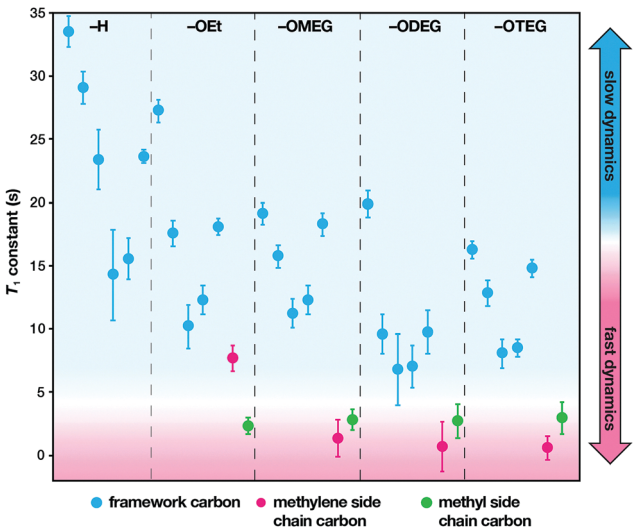

Fig. 3 T_1 spin–lattice relaxation constants for each carbon signal in all the prepared COFs. Framework carbon data (blue symbols) include aromatic, imine and carbonyl carbons. Error bars correspond to one standard deviation from the fitting.

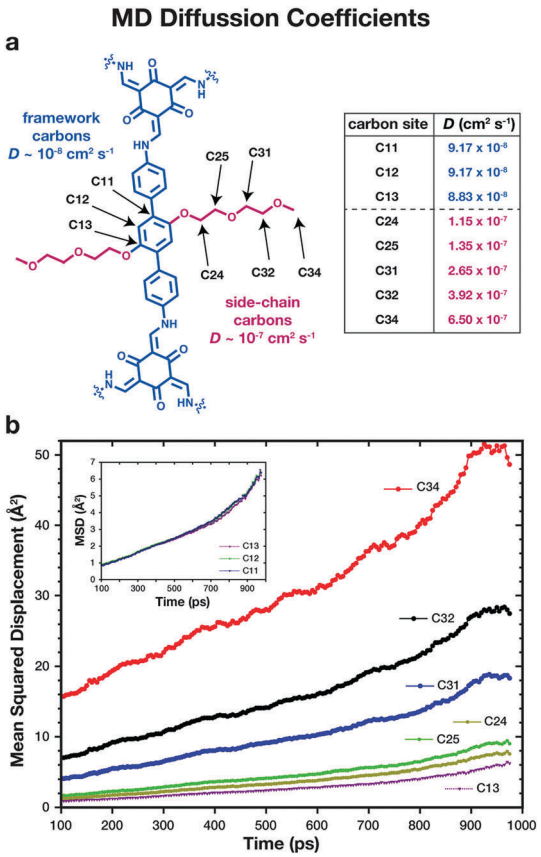

Fig. 4 Molecular dynamics (MD) simulation of **TfpTP-ODEG** at 298 K. (a) Carbon sites analysed summarizing their diffusion coefficients. (b) Mean square displacement (MSD) *vs.* time plot for each of the analysed atoms. Inset: MSD *vs.* time plot of framework carbons.

OTEG groups is roughly the same. We note that the longer side-chains of **ODEG** and **OTEG** appear to significantly enhance ^{13}C relaxation of the aromatic framework. These observations highlight the ability of COFs to exhibit amphidynamic behaviour which can be easily accessed and designed.

Molecular dynamics (MD) simulations were performed in LAMMPS[15] to further understand the different dynamics of the atoms composing the structures. The results for **TfpTP-ODEG** are shown in Fig. 4. The MD trajectories indicate the carbon atoms in the backbone have a smaller order of magnitude when compared to the carbon atoms in the side-chains (Fig. 4a). This is a similar finding to the NMR results. The MD results further show that the side-chains have apparent larger mean squared deviation (MSD) because the side chains can move back and forth and up and down inside the pore, which turns into a larger apparent diffusion coefficient (see the videos in the ESI†). The trajectories also show that this is not a pure classical Brownian motion. The ideal Brownian motion is expected as:

$$MSD \propto D{\cdot}t \qquad (2)$$

where D is the diffusion coefficient and t is time; however, there are regions in the trajectory of the side chains and the even the backbone atom that suggest anomalous diffusion. The details of this behaviour are beyond the scope of this work; nonetheless,

we were able to obtain the diffusion coefficient of the ideal region (Fig. 4b). Notice the order of order of magnitude difference between the side chains (10^{-7} cm^2 s^{-1}) *versus* the backbone carbons (10^{-8} cm^2 s^{-1}). This is to best of our knowledge the first time this behaviour is observed and characterized in a COF.

In summary, we prepared a family of covalent organic frameworks that have been functionalized with oligo-ethylene oxide side-chains to probe the differences in amphidynamic behaviour between the organic framework and the side-chain. We observed through solid-state NMR measurements that the crystalline COFs exhibit the expected amphidynamic behaviour allowing to probe the effects of the various functional groups systematically with easy synthesis methods. The MD simulations further show that the atomistic behaviour of the side chain is different than the backbone atoms, thus predicting different apparent diffusion coefficients. The values for the diffusion coefficient are in the range of Li diffusion in some graphite systems which makes them promising candidates for transport applications, especially as solid-state electrolytes for all-solid-state Li-ion batteries. Taking advantage of unique features in COFs—tuneable porosity, modularity, and predictability of crystal packing—can provide an insight to understanding how dynamic processes in organic solids can be controlled and designed.

FJU-R would like to acknowledge the UCF College of Sciences and Office of Research and Commercialization for funds, JKH would like to thank the National Science Foundation (grant no. CHE-14551592) for funds. JLM-C gratefully acknowledges support from the Energy and Materials Initiative at FSU for funds and its High-Performance Computer (HPC) for computational resources and support.

Conflicts of interest

There are no conflicts to declare.

Notes and references

‡ Although, polymorphism cannot be ruled out.

1 J. Michl and E. C. H. Skyes, *ACS Nano*, 2009, **5**, 1042–1048.
2 (*a*) I. Fischbach, T. Pakula, P. Minkin, A. Fechtenkotter, K. Mullen and H. W. Spiess, *J. Phys. Chem. B*, 2002, **106**, 6408–6418; (*b*) C. S. Vogelsberg and M. A. Garcia-Garibay, *Chem. Soc. Rev.*, 2012, **41**, 1892–1910; (*c*) U. Vovensiepen, H. Petek and M. Wolf, *Dynamics at Solid State Surfaces and Interfaces*, Wiley-VCH, 2012; (*d*) A. Credi, S. Silvi and M. Venturi, *Molecular Machines and Motors: Recent Advances and Perspectives*, Springer, 2014.
3 (*a*) Z. Dominguez, H. Dang, M. J. Strouse and M. A. Garcia-Garibay, *J. Am. Chem. Soc.*, 2002, **124**, 2398–2399; (*b*) Z. Dominguez, T.-A. V. Khuong, C. N. Sanrame, H. Dang, J. E. Nunezand and M. A. Garcia-Garibay, *J. Am. Chem. Soc.*, 2003, **125**, 8827–8837.
4 (*a*) J. Maddox, *Nature*, 1988, **335**, 201; (*b*) F. J. DiSalvo, *Science*, 1990, **247**, 649–655; (*c*) F. C. Hawthorne, *Nature*, 1990, **345**, 297.
5 (*a*) J. W. Colson and W. R. Dichtel, *Nat. Chem.*, 2013, **5**, 453–465; (*b*) P. J. Waller, F. Gándara and O. M. Yaghi, *Acc. Chem. Res.*, 2015, **48**, 3053–3063; (*c*) X. Chen, M. Addicoat, E. Jin, H. Xu, T. Hayashi, F. Xu, N. Huang, S. Irle and D. Jiang, *Sci. Rep.*, 2015, **5**, 14650.
6 (*a*) E. L. Spitler, J. W. Colson, F. J. Uribe-Romo, A. R. Woll, M. R. Giovino, A. Saldivar and W. R. Dichtel, *Angew. Chem., Int. Ed.*, 2012, **51**, 2623–2627; (*b*) X. Chen, M. Addicoat, E. Jin, H. Xu, T. Hayashi, F. Xu, N. Huang, S. Irle and D. Jiang, *Sci. Rep.*, 2015, **5**, 14650.
7 A. P. Côté, A. I. Benin, N. W. Ockwig, M. O'Keeffe, A. J. Matzger and O. M. Yaghi, *Science*, 2005, **310**, 1166–1170.
8 D. A. Vazquez-Molina, G. S. Mohammad-Pour, C. Lee, M. W. Logan, X. Duan, J. K. Harper and F. J. Uribe-Romo, *J. Am. Chem. Soc.*, 2016, **138**, 9767–9770; S. Panero, B. Scrosati and S. G. Greenbaum, *Electrochim. Acta*, 1992, **37**, 1533–1539.
9 S. Panero, B. Scrosati and S. G. Greenbaum, *Electrochim. Acta*, 1992, **37**, 1533–1539.
10 S. Kandambeth, A. Mallick, B. Lukose, M. V. Mane, T. Heine and R. Banerjee, *J. Am. Chem. Soc.*, 2012, **134**, 19524–19527.
11 S. Karak, S. Kandambeth, B. P. Biswal, H. S. Sasmal, S. Kumar, P. Pachfule and R. Banerjee, *J. Am. Chem. Soc.*, 2017, **139**, 1856–1862.
12 *Materials Studio, version 8.0*, BIOVIA Software Inc., San Diego, CA, 2014.
13 V. K. Pecharsky and P. Y. Zavalij, *Fundamentals of Powder Diffraction and Structural Characterization of Materials*, Springer, 2009.
14 X. Jiang, B. Rodríguez-Molina, N. Nazarian and M. A. Garcia-Garibay, *J. Am. Chem. Soc.*, 2014, **136**, 8871–8874.
15 S. Plimpton, *J. Comp. Physiol.*, 1995, **117**, 1–19.

